Chain Photoreduction of CCl_3F Induced by TiO_2 Particles

R. L. Calhoun, K. Winkelmann, and G. Mills*

Department of Chemistry, Auburn University, Auburn, Alabama 36849

Received: December 14, 2000; In Final Form: July 16, 2001

Fluorotrichloromethane (CFC 11) is dehalogenated through a reductive chain reaction upon illumination of aqueous, air-free suspensions of TiO_2 particles in the presence of formate ions. The reduction takes place with large photonic efficiencies at pH ≥ 5 even at high photon fluxes, producing mainly Cl^- and dichlorofluoromethane (HCFC 21), while F^- is only a minor byproduct. In the proposed mechanism $^{\bullet}CO_2^-$ and $^{\bullet}CCl_2F$ radicals are the chain carriers, Cl^- as well as HCFC 21 result from propagation steps, and cross-termination of the chain carriers forms F^-. Simple steady-state assumptions, that regard propagations as the dominant steps, yield kinetic equations consistent with the data of the initial fast Cl^- formation step. The subsequent evolution of rates and postirradiation effects are consequences of the slow removal of electrons from the semiconductor.

Introduction

Illumination of semiconductor particles in solution is a simple way to drive reactions of organic compounds with light. These processes have been investigated for photosynthetic purposes as well as for the elimination of undesirable compounds.[1−5] The photoreactions frequently involve free radicals generated when charge carriers or surface-trapped radicals attack substrate molecules located in the interfacial region.[6] Nonselective attack by the light-generated reactive species yields multiple products, as usually found during oxidations of organic halides.[3−5] Selective reduction of these compounds has been achieved under appropriate conditions, resulting in stepwise dehalogenations or complete hydrolysis.[7−9] In general low quantum efficiencies are typical of the phototransformations because of fast combination reactions of charge carriers or radicals. Exceptions occur when radical chain reactions are initiated,[10−12] or under conditions where efficient scavenging of charge carriers takes place as noticed during the photoreduction of Ag^+ ions induced by TiO_2 colloids in ethanol.[13]

Early radiation chemical investigations demonstrated that selective and efficient reductive dehalogenations of organic halides via radical chain reactions are possible in air-free homogeneous solutions.[14] Subsequent studies have shown that similar processes occur for a variety of compounds including fluorides and fluorohalides.[15−18] These results suggested that efficient dehalogenations were feasible via chain reductions initiated by irradiation of semiconductor particles. Such reactions seemed attractive for the transformation of chlorofluorocarbons (CFCs) into their hydrogen-substituted analogues (HCFCs), which currently replace them.[19] This idea was tested using CCl_2FCF_2Cl (CFC 113) and CCl_3CF_3 (CFC 113a).[20] Both Freons were photoreduced to HCFCs in air-free aqueous TiO_2 suspensions containing HCO_2^- ions; occurrence of efficient chain reductions was evident at low light intensities. Chain dehalogenations of CCl_4 in basic solution have been recently reported to take place faster than the dark hydrolysis reaction in suspensions containing alcohols as electron donors;[8a] higher efficiencies were obtained upon low-intensity illumination of TiO_2 films.[21]

The present study examined the photoreduction of CCl_3F (CFC 11), the largest contributor to the disruption of the stratospheric ozone cycle;[22] efforts were made to achieve efficient chain transformations of the Freon. Degassed suspensions of TiO_2 saturated with CCl_3F and containing high concentrations of HCO_2^- ions as electron donors were employed to initiate the photoreductions because oxidation of formate generates strongly reducing $^{\bullet}CO_2^-$ radicals.[23] These conditions were selected since, as was shown before,[20] they favor chain propagation steps and suppress unwanted reactions such as the complete dehalogenation of the chlorocarbon chain carriers.[8,9,21] The photoreduction of CCl_3F was found to be significantly faster than that of CCl_2FCF_2Cl, taking place through efficient chain reactions even at high light intensities.

Experimental Section

Reagent grade chemicals were obtained from Aldrich or Fisher and were not further purified. Water from a Milli-Q-Plus system (Millipore) was used in all preparations; occasionally the results were verified using HPLC water (Fisher). Suspensions of 0.5 g L^{-1} TiO_2 particles (Degussa P-25, 30 nm average diameter) were prepared inside photochemical reactors containing 110 mL of aqueous HCO_2H/HCO_2Na buffers. After the photoreactors were sealed, the suspensions were deaerated with Ar for 30 min under stirring. Liquid CCl_3F that had been degassed using three freeze−pump−thaw cycles was introduced into the photoreactors via airtight syringes. The Freon was injected directly into the suspensions to avoid extensive vaporization (bp = 23.8 °C). Stirring of the mixtures in the dark proceeded then for 10−30 min prior to illumination; the resulting kinetic data were independent of the length of this equilibration period.

Borosilicate glass vessels with an internal volume of 170 mL were employed as photoreactors. The vessels were constructed by flattening one curved side of a cylinder (70 mm internal diameter, 38 mm height, 2 mm wall thickness) to form a 51 mm × 38 mm window. These vessels were joined to slightly larger glass vessels (5 mm wall thickness) of the same shape to

* To whom correspondence should be addressed. E-mail: millsge@auburn.edu.

10.1021/jp004501i CCC: $20.00
Published on Web 09/19/2001

form water-jackets and to increase the strength of the photochemical reactors. Reinforcement of the photoreactors was considered mandatory because headspace pressures of 1.9 atm were measured (with an Ashcroft gauge) after injecting the CFC into the vessels. *Caution should be exercised while performing similar experiments because the photoreactors were shattered on a couple of occasions*. Three glass joints connected to the inner vessels were fused on top of the photoreactors. Perforated septa, through which tightly fitted electrodes were immersed into the suspension, served as seals for the glass joints. Since an opening exists on the top of the reference electrode, precautions were taken to avoid subjecting the electrode to pressure gradients and to eliminate diffusion of air into the suspensions. This was accomplished by pushing the electrode into the vessel until the opening was positioned in the headspace of the suspensions underneath the septa.

Irradiations were performed at 23 °C using a Thermix 120 MR stirrer to provide a constant stirring rate (320 rpm). Light from a PTI 1010 S system equipped with a 150 W Xe arc lamp was passed through a 10 cm water filter, an IR-absorbing filter, and a Kopp GS-7-60 filter. Photons in the range of $320 \leq \lambda \leq 385$ nm were selected and then focused onto the lateral window of the photoreactor. Adjustment of the intensity of light (I_0) was accomplished with neutral density filters; determinations of I_0 were performed for each kinetic run using the Aberchrome 540 actinometer.[24] The effectiveness of the photoreduction is given in terms of the photonic efficiency (P.E.), which corresponds to the formation rate of product divided by the rate of incident photons.[2] Photon losses due to light scattering by small CCl_3F droplets and by TiO_2 particles were not included in the calculation of P.E.

In general, the same methods and instrumentation of our previous study were employed for the in situ determination of Cl^-, F^-, and H^+ concentrations, as well as for GC−MS analysis of halocarbon products.[20] The halide ion-selective electrodes were calibrated in the dark prior to each experiment under conditions duplicating those of the kinetic runs. This procedure ensured that any halide ions adsorbed on the surface of the oxide were accounted for. Each experiment was performed at least twice; while deviation of the results was usually less than 20%, deviations of 30% were noticed occasionally. In the CCl_2FCF_2Cl system potentiometric data were acquired after interrupting the irradiation to avoid artificial photovoltages resulting from direct illumination of the electrodes.[20] Implementation of such a procedure was not possible in the present study because postirradiation reactions took place. Potentiometric determinations were carried out under continuous illumination with suspensions containing 0.5 g L^{-1} TiO_2 in all experiments. In addition to ensuring effective shielding of the electrodes from light, this concentration the oxide particles has yielded maximum efficiencies in a variety of photoreactions,[4] including reduction of Freons.[20] Furthermore, the ion-selective and reference electrodes were immersed in the suspensions via the two glass joints situated near the back of the photoreactors. Under these conditions blank experiments without CCl_3F indicated that the contribution of the photovoltages to the signal due to halide ion generation was negligible even during the slow induction period (less than 0.2%).

Results

The limiting solubility of CCl_3F in water is 8×10^{-3} M (82 μL of Freon in 110 mL solution),[25] and tests confirmed that this solubility limit was not altered by the buffer or the semiconductor particles. Unless otherwise stated, the suspensions always contained 2 mL CCl_3F. Two liquid phases were therefore present, and the oxide particles remained in the aqueous phase, which also contained numerous small Freon droplets generated upon stirring. Since no reduction of CCl_3F was detected in the absence of TiO_2, formation of halide ions must be attributed to processes taking place in the aqueous suspension phase. Although the Freon transformation generated H^+ ions, only slight pH decreases were noticed in the presence of the buffers. Throughout this study the buffer concentration is given in terms of $[HCO_2^-] + [HCO_2H]$. Volatile products generated in suspensions containing 0.3 M buffer (pH 5.9) irradiated for 1 h with $I_0 = 1 \times 10^{-6}$ M($h\nu$) s^{-1} were identified by means of GC−MS. $CHCl_2F$ (HCFC 21) and CO_2 were detected as products of the photoreaction, as well as traces of the CCl_2F_2 impurity present in some of the CCl_3F samples. Other possible halocarbon products, such as CH_2ClF, CCl_2F-CCl_2F, and $CClF{=}CClF$, were not found.

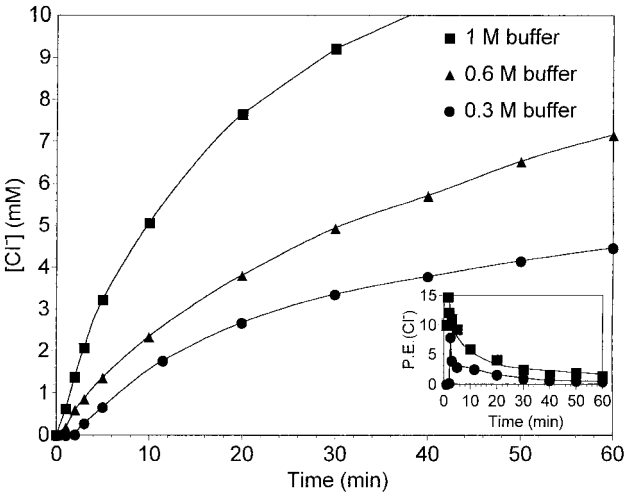

Figure 1. Plot of $[Cl^-]$ vs time for Ar-saturated suspensions containing 0.5 g L^{-1} TiO_2, 2 mL of CFC 11, illuminated with $I_0 = 1 \times 10^{-6}$ M($h\nu$) s^{-1} at pH = 5.9 in the presence of $[HCO_2^-] = 0.3$ (●), 0.6 (◆), and 1 M (■). Inset: evolution of P.E.(Cl^-) as a function of time for $[HCO_2^-] = 0.3$ (●) and 1 M (■).

Presented in Figure 1 is the evolution of $[Cl^-]$ as a function of time for suspensions saturated with CFC at pH 5.9 containing 1, 0.6, and 0.3 M HCO_2H/HCO_2Na buffer. All reactions proceeded via two steps: an initial induction period lasting 0.5−2 min, where $[Cl^-]$ changed slowly, followed by a step where Cl^- ion generation was at least 5 times faster. The length of the induction period was not reproducible and, with the exception of low I_0 values, was independent of pH, concentrations of reactants, and degassing or equilibration times. During this period Cl^- ions (and F^-) were generated in very small amounts through processes obeying no simple rate law. Hence, the kinetic data of this step were not further analyzed. As seen in Figure 1, $[Cl^-]$ increased rapidly at the early stages of the second step but the chloride formation rate decreased at longer times. Nevertheless, Cl^- concentrations higher than 9×10^{-3} M were reached at 30 min in systems with 1 M buffer. Efforts to fit the results according to a first-order rate law were unsuccessful.

Rates of Cl^- generation, $r(Cl^-)$, derived from the data of the second step were employed to calculate the photonic efficiency of Cl^- formation, P.E.(Cl^-). Depicted in the inset of Figure 1 are the variations of P.E.(Cl^-) during reactions in the presence of 1 and 0.3 M buffer. $[Cl^-]$ increased linearly with time during the first minute of the second step where $r(Cl^-)$ reached a maximum value, denoted as the initial formation rate, $r(Cl^-)_i$.

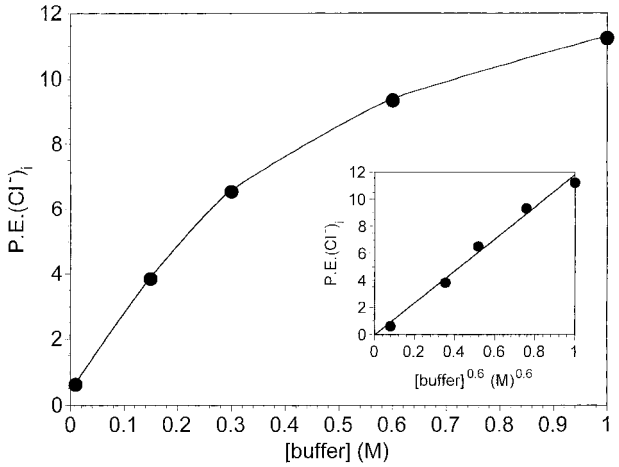

Figure 2. Variation of P.E.$(Cl^-)_i$ with buffer concentration in systems at pH = 5.9 with 0.5 g L^{-1} TiO_2, 2 mL of CCl_3F, and $I_0 = 1.6 \times 10^{-6}$ M($h\nu$) s^{-1}. Shown in the inset is the linear relationship between P.E.$(Cl^-)_i$ and $[buffer]^{0.6}$.

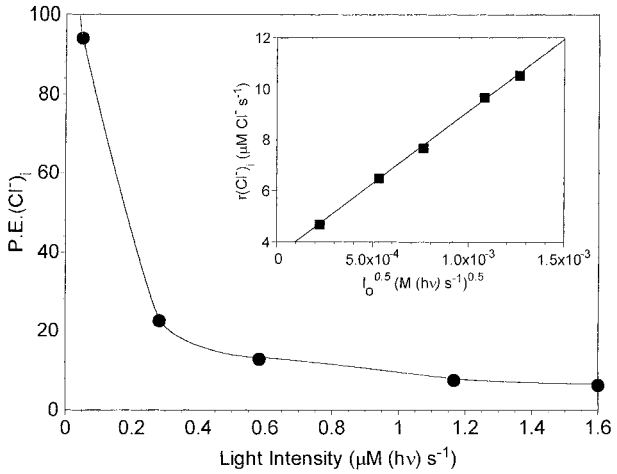

Figure 3. Dependence of P.E.$(Cl^-)_i$ on light intensity in suspensions at pH 5.9 containing 0.5 g L^{-1} TiO_2, 0.3 M buffer, and 2 mL of CFC 11. Presented in the inset is the evolution of $r(Cl^-)_i$ with $(I_0)^{0.5}$.

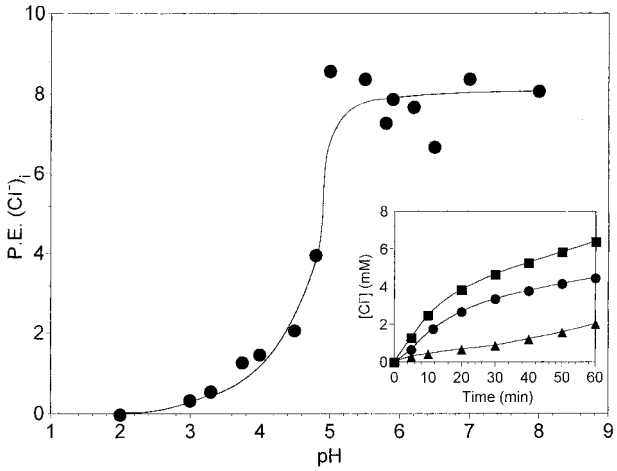

Figure 4. Changes in P.E.$(Cl^-)_i$ as a function of pH for suspensions with $[HCO_2^-] + [HCO_2H] = 0.3$ M and 2 mL of CFC 11, 0.5 g L^{-1} TiO_2, $I_0 = 1.1 \times 10^{-6}$ M ($h\nu$) s^{-1}. The inset shows the change in $[Cl^-]$ with photolysis at pH 4 (▲), pH 5.9 (●), and pH 8 (■).

Initial photonic efficiencies, P.E.$(Cl^-)_i$, obtained from these maximum rates were used to characterize the photoreduction kinetics of CCl_3F. The evolution of $[F^-]$ during the second step was similar to that of $[Cl^-]$; the corresponding maximum rates of F^- generation were employed to calculate the initial photonic efficiencies, P.E.$(F^-)_i$. However, as will be shown later, the fluoride concentrations were much smaller than the Cl^- concentrations.

Figure 2 illustrates the dependence of P.E.$(Cl^-)_i$ on the concentration of the formate buffer. The experiments were performed at pH 5.9 using the highest light intensity available, $I_0 = 1.6 \times 10^{-6}$ M($h\nu$) s^{-1}. A continuous increase of P.E.$(Cl^-)_i$ was observed when the electron donor concentration was raised, reaching a value of P.E.$(Cl^-)_i = 11.3$ at 1 M formate. As shown in the inset, P.E.$(Cl^-)_i$ is linearly related to the buffer concentration raised to the power of 0.6. It should be noted that a straight line was also obtained from a plot of the reciprocal of P.E.$(Cl^-)_i$ vs $[buffer]^{-1}$. However, the large values of P.E.$(Cl^-)_i$ presented in Figures 1 and 2 clearly demonstrate that the photoreduction of CCl_3F is a chain reaction. Therefore, data analysis within the framework of chain processes was preferred because several different mechanisms yield linear relationships between $(rate)^{-1}$ and the reciprocal of [substrate].[5,26] At reaction times longer than 30 min the dependency of the photonic efficiencies on [buffer] changed, increasing linearly as the concentration of formate was augmented.

Depicted in Figure 3 is the variation of P.E.$(Cl^-)_i$ with I_0 for systems at pH 5.9 with 0.3 M buffer. The initial photonic efficiency decreased from 95 to 6.9 when the light intensity increased from 5.2×10^{-8} to 1.6×10^{-6} M($h\nu$) s^{-1}. Because the formation rate of product is related to I_0 in a simpler way than P.E.$(Cl^-)_i$, it is useful to present the results of Figure 3 in terms of $r(Cl^-)_i$. As shown in the inset, the initial rate is a linear function of the square root of the light intensity. While the length of the induction period was, in most cases, not dependent on I_0, this period increased by a factor of 4 at the lowest light intensity used in this study.

Values of P.E.$(Cl^-)_i$ as a function of pH were obtained at a constant buffer concentration of 0.3 M and varying ratio $[HCO_2^-]/[HCO_2H]$. At pH > 8 the high formate concentration caused interferences in the operation of the ion-selective electrodes. Therefore, determinations of P.E.$(Cl^-)_i$ were limited to pH ≤ 8; the results are summarized in Figure 4. P.E.$(Cl^-)_i$ increased steadily from 0.01 to 2 between pH 2 and pH 4.5, followed by a sharp increase to reach an average value of 7.9 in the range 5 ≤ pH ≤ 8. The inset shows the evolution of $[Cl^-]$ as a function of time for experiments with pH = 8, 5.9, and 4. Values of P.E.$(Cl^-)_i$ equal to 8.2, 7.9, and 1.4 resulted at these three different $[H^+]$ concentrations, and the corresponding P.E.$(F^-)_i$ values were 0.19, 0.18, and 0.14. The initial fast chloride ion formation at pH ≥ 5.9 turned progressively slower as illumination proceeded. For instance, $r(Cl^-)$ declined in the first 10 min of photolysis from 7.9×10^{-6} to 1.9×10^{-6} M s^{-1} at pH = 5.9 and from 8.3×10^{-6} to 3.7×10^{-6} M s^{-1} at pH = 8. In contrast, at pH 4 the formation rate of chloride ions increased with time of exposure, reaching a rate similar to those measured at higher pH values after about 6 h.

Experiments were also carried out at various pH values in systems containing reaction products. Within experimental error, P.E.$(Cl^-)_i$ was not affected by the presence of up to 1 mM Cl^- throughout the pH range studied. Below pH 5.9 no effect of F^- on P.E.$(Cl^-)_i$ was found, but at pH ≥ 5.9 efficiencies about 40% higher than those of Figure 4 were measured when $[F^-]$ ≥ 10 μM. Similar high P.E.$(Cl^-)_i$ values were determined in systems free of F^-, employing a modified method to exclude air from the suspensions. In this method the HCO_2^- buffers were deaerated prior to introduction of the TiO_2 powder into the photoreactors, which hindered any adsorption of CO_2 present

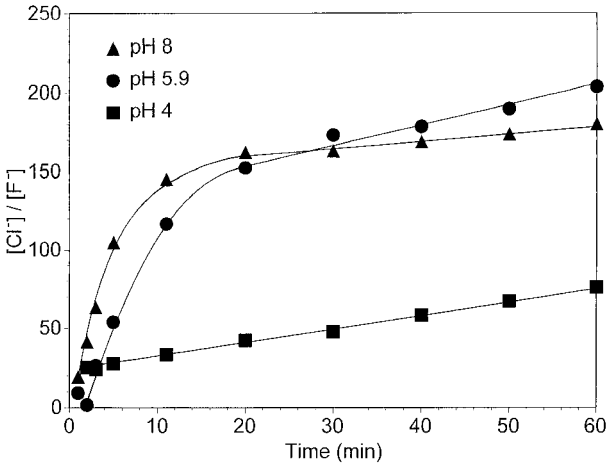

Figure 5. Variation of the ratio $[Cl^-]/[F^-]$ during illumination of air-free systems with 0.3 M buffer, 0.5 g L^{-1} TiO_2, and 2 mL of CCl_3F at pH 4 (■), pH 5.9 (●), and pH 8 (▲).

in air onto the wet semiconductor surface. However, the same results of Figure 4 were obtained when the modified degassing method was followed by addition of up to 0.14 mM $NaHCO_3$ (pH changes occur at higher concentrations). Thus, HCO_3^- decreased the effectiveness of the fast step, probably by binding to the oxide surface and acting as a center for charge carrier recombination. This implies that F^- ions, which are not attacked by charge carriers, suppressed the inhibiting effect of HCO_3^- ions probably by displacing them from the oxide surface. While F^- increased $r(Cl^-)_i$ only, carbonate decreased P.E.$(Cl^-)_i$ but enhanced chloride generation at longer times. After the initial step, the curve of $[Cl^-]$ vs time for a suspension containing HCO_3^- at pH 5.9 increasingly diverged from the corresponding curve shown in the inset of Figure 4, approaching the curve of pH 8.

Illustrated in Figure 5 are the concentration ratios of Cl^- and F^- that correspond to the kinetic data of the inset in Figure 4. For presentation purposes only the results of the early stages at pH 5.9 were included. In this experiment the induction period lasted 2 min, during which $[Cl^-]/[F^-]$ fluctuated between 3 and 7. This ratio increased abruptly to 26 during the fast initial Cl^- formation of the second step; ratios of 19 and 15 were obtained for pH = 8 and 4, respectively. The concentration ratio continued to increase within the first 10 min at pH $\geq$ 5.9, followed by smaller increases thereafter. On the other hand, $[Cl^-]/[F^-]$ increased linearly as the reaction proceeded at pH = 4. The ratios of rates $r(Cl^-)/r(F^-)$, which correspond to the kinetic chain lengths, yielded curves resembling those of Figure 5 when plotted vs time. However, the ratios of formation rates were much higher than the ratios of concentrations, with initial values of 43.9 at pH 5.9 and 43.2 at the higher pH. Despite of the decreases in $r(Cl^-)$ as photolysis proceeded, larger declines of $r(F^-)$ were noticed. For example, at pH = 5.9 this rate fell from 2×10^{-7} to 6.1×10^{-9} M s^{-1} after 10 min. Thus, during this time the ratios of $r(Cl^-)/r(F^-)$ increased to 311 and 292 at pH 5.9 and 8, respectively, and then slowly to about 460 after 1 h. For pH 4 the ratio was initially 10 but changed to 63 within 10 min followed by a linear increase to 130 after 60 min.

Several additional experiments were carried out at pH 5.9 with 0.3 M buffer and $I_0 = 1 \times 10^{-6}$ M($h\nu$) s^{-1}. Experiments with a Freon volume of 4 mL yielded initial photonic efficiencies identical to the value obtained with 2 mL. Postirradiation reactions lasted in air-free suspensions between 0.5 and 1 h and generated both halide ions with $[Cl^-]/[F^-] \gg 3$. In air-saturated sealed suspensions, formation of both halide ions was slow for more than 15 min, with a P.E.(Cl^-) value lower (0.02) than those of the induction period in degassed samples (0.06−0.2). Photolysis of a system saturated with $CHCl_2F$, the halocarbon product of the CCl_3F reduction, resulted in a linear change of $[Cl^-]$ as a function of time with P.E.$(Cl^-) = 0.05$. HCFC 21 has a limiting solubility of 0.093 M,[25] which was achieved by degassing suspensions with this halocarbon (bp = 8.9 °C).

Discussion

The data gathered in the present investigation indicates that CCl_3F is reduced in illuminated air-free TiO_2 suspensions containing HCO_2^- ions, producing Cl^- ions and $CHCl_2F$ as the main products. Occurrence of a slow induction period preceding the fast reduction step is not unexpected since traces of air are inevitably introduced into the suspensions during injection of CCl_3F. The low P.E.(Cl^-) values and the $[Cl^-]/[F^-]$ ratios much smaller than during the second step indicate that no chain reaction of CCl_3F takes place during this period. Similar observations were made in air-saturated systems, confirming that the induction period originates from the presence of small amounts of O_2 in the suspensions. Freon reduction predominates after most of the oxygen is consumed, at which point Cl^- starts forming fast. Reaction rates higher than the formation rate of initiating species and O_2-induced inhibitions are typical features of radical chain reactions,[10,11,14−18] including the photoreduction of CFC 113 induced by TiO_2 particles.[20] The high photonic efficiencies of Cl^- formation (Figures 1−4) and the inhibiting effect of air are evidence that the reduction of CCl_3F occurs through an analogous radical chain process.

Significant differences exist, however, between the reactions of CCl_3F and CCl_2FCF_2Cl because in suspensions with 0.3 M HCO_2^- at pH = 6 and $I_0 = 1 \times 10^{-6}$ M($h\nu$) s^{-1} induction periods 4 times shorter and P.E.$(Cl^-)_i$ values 14 times higher occur for CFC 11. Also, postirradiation reduction occurs only in the CCl_3F system, meaning that the kinetic chain length is much longer for this CFC. Studies of photopolymerizations initiated by semiconductor particles have shown that radical chain processes are inefficient at low [substrate].[10] Thus, the dissimilar behavior of the two Freons is related, in part, to the fact that in a solution saturated with CCl_3F the [CFC] is about 9 times higher than the solubility limit of CFC 113. Also, $E^0(CCl_3F/^\bullet CCl_2F,Cl^-)$ was estimated to be −0.44 V,[23] whereas the half-wave potential for CFC 113 is −1.21 V.[27] Reaction of $^\bullet OH$ radicals or holes with HCO_2^-/HCO_2H located on or next to the TiO_2 surface yields $^\bullet CO_2^-$ radicals,[28] which are the most powerful reductants in the suspensions ($E^0 = -1.8$ V for $CO_2/^\bullet CO_2^-$).[23] From these redox potentials it is reasonable to expect the reduction of CCl_3F by $^\bullet CO_2^-$ radicals to be more efficient than the analogous reaction of CFC 113. Participation of $^\bullet CO_2H$ in the CCl_3F reduction is not significant because a pH > 2 was used in most experiments, whereas the pK_a is 1.4 for this radical.[23]

Earlier studies have shown that $^\bullet CO_2^-$ radicals are involved in the homogeneous chain reductions of CF_3I, CF_3Br, and $CF_3CHBrCl$ that form I^- or Br^- and hydrogen-substituted derivatives (CHF_3 and CF_3-CH_2Cl).[15,17a] The results of Figure 2 confirm that HCO_2^- participates in the chain process, and the plot shown in the inset is concordant with mechanisms implicating the radicals of the electron donor.[29] A linear variation of the reaction rate with $(I_0)^{0.5}$ is predicted by these mechanisms, which agrees fairly well with the relationship presented in the inset of Figure 3. Also, CO_2 was detected by GC−MS, which is the anticipated product when $^\bullet CO_2^-$ acts as a reductant. These kinetic features along with the main reaction products suggest

that the CCl_3F reduction mechanism is similar to those of homogeneous chain processes. The following sequence of elementary steps is consistent with the kinetics of the CCl_3F photoreduction:

$$TiO_2 + h\nu \rightarrow h_{vb}^{+} + e_{cb}^{-} \quad (1)$$

$$h_{vb}^{+} + e_{cb}^{-} \rightarrow \text{heat} \quad (2)$$

$$h_{vb}^{+} + H_2O \rightarrow {}^{\bullet}OH + H^{+} \quad (3)$$

$$h_{vb}^{+}/{}^{\bullet}OH + HCO_2^{-} \rightarrow {}^{\bullet}CO_2^{-} + H^{+}/H_2O \quad (4)$$

$${}^{\bullet}CO_2^{-} + TiO_2 \rightarrow e_{cb}^{-} + CO_2 \quad (5)$$

$$e_{cb}^{-} + CCl_3F \rightarrow {}^{\bullet}CCl_2F + Cl^{-} \quad (6)$$

$${}^{\bullet}CO_2^{-} + CCl_3F \rightarrow {}^{\bullet}CCl_2F + Cl^{-} + CO_2 \quad (7)$$

$${}^{\bullet}CCl_2F + HCO_2^{-} \rightarrow {}^{\bullet}CO_2^{-} + HCCl_2F \quad (8)$$

$${}^{\bullet}CCl_2F + {}^{\bullet}CO_2^{-} \rightarrow :CClF + Cl^{-} + CO_2 \quad (9)$$

$${}^{\bullet}CCl_2F + e_{cb}^{-} \rightarrow :CClF + Cl^{-} \quad (10)$$

$$:CClF + 2H_2O \rightarrow HCO_2^{-} + HCl + HF + H^{+} \quad (11)$$

Trihalomethyl radicals ($^{\bullet}CX_3$) are important intermediates during the transformation of $CHCl_3$, $CHBr_3$, and CCl_4 in TiO_2 suspensions.[8,9] These radicals undergo reductions analogous to steps 9 and 10 to form carbenes ($:CX_2$) or dimerize to CX_3-CX_3. Carbenes can either dimerize to $CX_2=CX_2$ or hydrolyze producing HCO_2^{-}/CO and HX in a reaction similar to step 11. Chain transformations of CCl_4 in basic solutions containing alcohols take place on illuminated TiO_2 suspensions and films.[8,21] The kinetic data were interpreted in terms of redox and hydrolytic reactions of the $^{\bullet}CCl_3$ radicals in solution or on the oxide surface. However, the finding that reduction of CCl_3F yields $CHCl_2F$ is inconsistent with mechanisms where hydrolysis is the main pathway.[8,9a,21] Furthermore, Figure 5 shows that $[Cl^{-}]/[F^{-}] \gg 3$, whereas such mechanisms predict formation of three Cl^{-} ions per F^{-} ion. The reactivity of $^{\bullet}CO_2^{-}$ radicals toward halocarbons is known to be higher than that of alcohol radicals;[15,17] the net result is a faster propagation (step 7) in our system, which reduces the chances of termination step 9. Since fluoride generation through hydrolytic step 11 is limited by steps 9 and 10, faster propagation steps reduce the efficiency of the hydrolysis. The fact that F^{-} is produced much slower than Cl^{-} and the persistent postirradiation effects that arise from the long chains are evidence that propagations predominate over terminations in the presence of HCO_2^{-}.

Slow terminations occur when the steady-state concentrations of $^{\bullet}CO_2^{-}$ and $^{\bullet}CCl_2F$ are low, which suppresses radical dimerizations and/or cross-terminations and decreases the steady-state concentration of :CClF. This explains the lack of signals from the CCl_2F-CCl_2F and CClF=CClF dimers when the suspensions were analyzed by GC−MS. Our results have shown that $CHCl_2F$ (the product of the CFC 11 reduction) is reduced much slower than CCl_3F; the fact that CH_2ClF was not found implies that $CHCl_2F$ is unable to compete with CCl_3F for the reductants in the suspensions. Findings from the radiolytic reduction of CCl_3F have been interpreted in terms of a hydrolysis step of $^{\bullet}CCl_2F$ radicals ($t_{1/2} = 15\ \mu s$) to form $^{\bullet}CClFOH$, followed by a further hydrolytic step with $t_{1/2} = 1.7$ s.[30] Interestingly, very similar reactions take place in the decay of CCl_3OH,[31] but such processes have not been observed for $^{\bullet}CCl_3$ radicals.[17b] H abstraction from HCO_2^{-} by $^{\bullet}CClFOH$ is anticipated to form CHClFOH, a species expected to hydrolyze producing both Cl^{-} and F^{-} and leading to $[Cl^{-}]/[F^{-}] = 3$. On the basis of the reasons given above, the proposed hydrolysis of $^{\bullet}CCl_2F$ radicals is inconsistent with the data of the present study and was not further considered.

Depending on $[H^{+}]$, some of these steps in the mechanism occur either on or next to the TiO_2 surface, which is positively charged below the pH of zero surface charge (pzc, ~6.2 for P-25)[32] and carries net negative charges above pzc. Binding of carboxylate ions ($R-CO_2^{-}$) to the oxide surface takes place below this pH; ion adsorption reaches a minimum at pzc, followed by preferential binding of the counterions to the surface at pH > pzc.[33] When $[R-CO_2Na] \geq 0.1$ M, the amounts of ions bound below and above pzc are significant and similar due to compression of the double layer. Therefore, a large amount of bound HCO_2^{-} exists between pzc and the pK_a of HCO_2H (3.75), binding of the acid predominates at pH < pK_a and was not included in the mechanism because a pH ≥ 4 was used in most cases. It follows that at pH < 6.2 step 4 comprises adsorbed HCO_2^{-}/HCO_2H, whereas above pzc this step involves HCO_2^{-} ions present in the double layer away from the surface. However, P.E.$(Cl^{-})_i$ is highest and constant at pH ≥ 5 (Figure 4), implying that HCO_2^{-} adsorption on the TiO_2 surface is not a controlling factor of the photoreaction.

At pH < 6.2 step 4 is a surface reaction generating adsorbed $^{\bullet}CO_2^{-}$ radicals, whereas above pzc the radicals form away (and are repelled) from the negatively charged surface. However, the data of Figure 4 imply that subsequent steps 7 and 8 are unaffected by changes in $[H^{+}]$ at pH ≥ 5. This means that the rates of the CCl_3F reduction by either free or bound $^{\bullet}CO_2^{-}$ are similar and that changes in the surface $[HCO_2^{-}]$ have no effect on the reaction of $^{\bullet}CCl_2F$ with formate. Since Freon adsorption on the oxide is not significant (the solubility of CCl_3F is unaffected by TiO_2), steps 6 and 7 must involve CFC molecules located next to the surface. The resulting $^{\bullet}CCl_2F$ radicals can diffuse and react with HCO_2^{-} ions present in the double-layer region; pH changes have no effect on this transformation because step 8 is not a surface reaction. After $^{\bullet}CCl_2F$ radicals are generated by light, the ensuing chain reduction proceeds mainly within the double layer through alternation of steps 7 and 8. On the basis of these conclusions, kinetic equations were derived using standard steady-state methods for homogeneous chain reactions based on the following approximations:[29] (a) the radical chains are long; (b) initiation is rate-determining and the rates of initiation and termination are equal; (c) the rates of all propagation steps are equal and much higher than the termination rate.

Because propagation occurs at some distance from the oxide surface and is faster than termination, the contributions of step 6 as well as of steps 9 and 10 to the overall generation rate of Cl^{-} are negligibly small. Also, the amount of Cl^{-} formed via step 11 (twice the amount of F^{-}) is insignificant compared to the contribution of step 7 because $[Cl^{-}] \gg [F^{-}]$ (Figure 5). These simplifications reduce the initial rate of Cl^{-} formation to the rate of step 7:

$$r(Cl^{-})_i = k_7[{}^{\bullet}CO_2^{-}][CCl_3F] \quad (12)$$

According to the above mechanism, P.E.$(Cl^{-})_i > 2$ is expected if the chain reaction occurs with steps 1 and 4 being 100% efficient. However, the effective photonic efficiencies of initia-

tion steps 1 and 4 are not known since these quantities are related to the fluxes of e_{cb}^- and $^\bullet CO_2^-$ radicals that actually survive steps 2 and 5 and react with the CFC. Because these fluxes are needed to test the validity of the proposed mechanism, an "effective" photonic efficiency of initiation, ζ_i, will be used instead. This quantity is equal to the total number of e_{cb}^- and $^\bullet CO_2^-$ radicals per photon that are able to react with CCl_3F. Because the number of e_{cb}^- that survive step 2 is equal to the number of h_{vb}^+, it is expected that equal numbers of electrons and $^\bullet CO_2^-$ radicals are initially available to react with CCl_3F. The photonic efficiency of initiation is also related to the rate of initiation, r_i, and under steady-state conditions r_i must be equal to the rate of termination step 9 (r_9). Step 10, a steady-state [:CClF] is reached when r_9 is equal to the rate of step 11 (r_{11}), and since the latter corresponds to the initial rate of F^- formation, $r(F^-)_i$, then $r(F^-)_i = r_i$. According to Figure 1, after 30 min $[Cl^-] > 9 \times 10^{-2}$ M for suspensions containing 1 M HCO_2^-, which is higher than the "molar concentration" of TiO_2 formula units (6.3×10^{-3} M). Thus, the oxide acts as a sensitizer that is not consumed during the photoreaction, implying that the rate of photons absorbed by the particles and r_i should be invariant with time. Consequently, $r_i = \zeta_i I_0$ or $r(F^-)_i = \zeta_i I_0$, and since $P.E.(F^-)_i = r(F^-)_i/I_0$, this results in $P.E.(F^-)_i = \zeta_i$, which at pH 5.9 is 0.18.

Once steady state is reached, the rates of propagation steps 7 and 8 (r_7 and r_8) must be equal, which together with $r_i = r_9$ results in

$$[^\bullet CO_2^-]_{ss} = \left(\frac{k_8 \zeta_i I_0}{k_7 k_9}\right)^{0.5} \left(\frac{[HCO_2^-]}{[CCl_3F]}\right)^{0.5} \tag{13}$$

where k_7, k_8, and k_9 are the rate constants of the corresponding elementary steps and $[^\bullet CO_2^-]_{ss}$ is the steady-state concentration of $^\bullet CO_2^-$. The rate law for the initial formation of Cl^- is obtained by combining eqs 12 and 13,

$$r(Cl^-)_i = \left(\frac{k_7 k_8 \zeta_i I_0}{k_9}\right)^{0.5} ([HCO_2^-][CCl_3F])^{0.5} \tag{14}$$

Equation 14 predicts a linear variation of $r(Cl^-)_i$ with both $[HCO_2^-]$ and I_0 raised to the power 0.5, agreeing well with the dependencies presented in Figures 2 and 3. A similar dependence of $r(Cl^-)_i$ with $[CCl_3F]$ is predicted by the rate law. No attempts were made to confirm this relationship because fast chain propagation is not expected to occur at low [CFC], altering the rate law.[29] In fact, data from photopolymerizations and from the reduction of CFC 113 have demonstrated that efficient radical chain reactions are not sustained when the substrate concentration is low.[10,20] Therefore, excess CCl_3F was used to ensure that $[CCl_3F]$ was constant and equal to the limit of solubility during the initial Cl^- generation step. Experiments with twice the usual Freon volume verified that this is the case since the reduction efficiency was the same as with 2 mL CCl_3F. Because direct confirmation of the rate law was not feasible, efforts were made to substantiate the validity of eq 14 by numerical means.

Although k_9 is not known, a rate constant of 1×10^9 M^{-1} s^{-1} has been frequently employed for the dimerization reaction of $^\bullet CO_2^-$ [17a] or $^\bullet CX_3$ radicals.[18b] Assuming a similar value for k_9, then step 9 predominates over the dimerizations of $^\bullet CO_2^-$ and $^\bullet CCl_2F$ when the chain carriers are formed not far away from each other and $[^\bullet CO_2^-]_{ss} \approx [^\bullet CCl_2F]_{ss}$, where $[^\bullet CCl_2F]_{ss}$ is the steady-state concentration of $^\bullet CCl_2F$. This approximation together with $r_7 = r_8$ yields $k_7/k_8 = [HCO_2^-]/[CCl_3F] = 37.5$; equations for the propagation rate constants are obtained by combining this expression with eq 14:

$$k_7 = \left(\frac{k_9}{\zeta_i I_0}\right)^{0.5} \frac{r(Cl^-)_i}{[CCl_3F]} \tag{15}$$

$$k_8 = \left(\frac{k_9}{\zeta_i I_0}\right)^{0.5} \frac{r(Cl^-)_i}{[HCO_2^-]} \tag{16}$$

Values of $k_7 = 6.8 \times 10^4$ M^{-1} s^{-1} and $k_8 = 1.9 \times 10^3$ M^{-1} s^{-1} are computed with the kinetic data of pH 5.9; $r(Cl^-)_i = 7.9 \times 10^{-6}$ M s^{-1}, $r(F^-)_i = 2 \times 10^{-7}$ M s^{-1} or $\zeta_i = 0.18$, $I_0 = 1.1 \times 10^{-6}$ M($h\nu$) s^{-1}, $k_9 = 1 \times 10^9$ M^{-1} s^{-1}, $[CCl_3F] = 8 \times 10^{-3}$ M, and $[HCO_2^-] = 0.3$ M. Evaluation of the steady-state concentrations of the chain carriers requires an independent expression other than eq 13. The kinetic chain length is equal to r_7/r_9, but $r_7/r_9 = r(Cl^-)_i/r(F^-)_i$ because, as shown above, $r_9 = r_{11}$, which results in the following expression:

$$[^\bullet CCl_2F]_{ss} = \frac{k_7[CCl_3F]\, r(F^-)_i}{k_9\, r(Cl^-)_i} \tag{17}$$

When $P.E.(Cl^-)_i/P.E.(F^-)_i = r(Cl^-)_i/r(F^-)_i = 43.9$ at pH 5.9 is used, eqs 13 and 17 yield $[^\bullet CO_2^-]_{ss} = 1.4 \times 10^{-8}$ M and $[^\bullet CCl_2F]_{ss} = 1.2 \times 10^{-8}$ M, agreeing well with the assumption that the chain carrier concentrations are very close. From the data at pH 8 ($r(F^-)_i = 2.1 \times 10^{-7}$ M s^{-1} or $\zeta_i = 0.19$, $P.E.(Cl^-)_i/P.E.(F^-)_i = 43.2$, $r(Cl^-)_i = 8.3 \times 10^{-6}$ M s^{-1}), the calculated kinetic parameters are $k_7 = 7.2 \times 10^4$ M^{-1} s^{-1}, $k_8 = 1.9 \times 10^3$ M^{-1} s^{-1}, $[^\bullet CO_2^-]_{ss} = 1.4 \times 10^{-8}$ M, and $[^\bullet CCl_2F]_{ss} = 1.3 \times 10^{-8}$ M. Having in mind that the derivation of eqs 12−17 was based only on standard steady-state assumptions used for chain reactions,[29] the calculated results provide further support for the proposed mechanism.

Procedures that attempt to account for the scattering of light by the oxide particles have been suggested.[34] One of the proposed methods (which increases ζ_i, $P.E.(Cl^-)_i$, and $P.E.(F^-)_i$ by a factor of 5.6) applies only for single-wavelength illuminations (365 nm); the other is based on kinetic features typical of oxidations of adsorbed reactants. Neither of these procedures were used systematically as they are unable to correct the light-scattering effects induced by the Freon droplets. Worth mentioning is that the term $\zeta_i I_0$ is included in eqs 13, 15, and 16, but since $\zeta_i = r_i/I_0$, then the calculated values of k_7, k_8, $[^\bullet CO_2^-]_{ss}$, and $[^\bullet CCl_2F]_{ss}$ are independent of I_0 and are not affected by photon losses due to scattering of light. Although k_8 is close to the rate constant for the homogeneous reaction between $^\bullet CHClCF_3$ and HCO_2^-, 2.9×10^3 M^{-1} s^{-1}, the average value of k_7, 7×10^4 M^{-1} s^{-1}, is 10^3 times smaller than the rate constant for the homogeneous reduction of halothane $CF_3CHBrCl$ by $^\bullet CO_2^-$ (7.6×10^7 M^{-1} s^{-1}).[17a] Because $^\bullet CO_2^-$ radicals are expected to react with CCl_3F as fast as they do with $CF_3CHBrCl$, the low k_7 value may reflect a decrease in the radical mobility due to ion pairing coupled with a $[CCl_3F]$ in the double layer smaller than the solubility limit of the Freon in water.

As is evident from Figure 4, significant decreases in the efficiencies of the reduction take place below pH 5. Also, the calculation of k_7 and k_8 using the data of pH 4 produced results divergent from those obtained at higher pH. The reason for this difference is that $P.E.(F^-)_i$ drops only by 22% upon changing the pH from 5.9 to 4 but $P.E.(Cl^-)_i$ decreases by more than 5 times. Obviously, the chains are shorter at the higher $[H^+]$, yielding lower ratios of $[Cl^-]/[F^-]$ (Figure 5). The trend

illustrated in Figure 4 is not unexpected because $^{\bullet}CO_2^-$ can reduce CCl_3F easily ($E^0_7 = 1.36$ V), whereas the flat-band potential of e_{cb}^- is pH-dependent, $E_{fb} = E^0_{fb} - (0.059)(pH)$.[35] The pH-corrected potential for step 6 ($E'_6 = E_{fb} - 0.44$ V) can then be utilized to estimate nonstandard potentials employing the Nernst equation, $E_6 = E'_6 - (RT/F)\ln Q$, with $Q = [Cl^-][^{\bullet}CCl_2F]_{ss}/([e_{cb}^-][CCl_3F])$. Electrons inside TiO_2 are known to persist for some time even when O_2 is present,[36] and in suspensions of P-25 containing formate, their decay is completed in about 1.5 s.[37] Thus, E_6 can be evaluated from the data gathered immediately after the induction period. Since a higher driving force is required to reduce the CFC, $E^0(O_2/O_2^-) = -0.16$ V,[23] the fraction of photogenerated e_{cb}^- that decay within 1 s of illumination is probably small. During this time $[e_{cb}^-] = 0.5\zeta_i I_0 = 9.9 \times 10^{-8}$ M (the factor 0.5 accounts for the similar contributions of e_{cb}^- and $^{\bullet}CO_2^-$ to ζ_i). As Figure 1 indicates, at the beginning of the fast step $[Cl^-] \approx 1 \times 10^{-4}$ M for 0.3 M HCO_2^-, which together with $E'_6 = -0.05$ V results in $E_6 = 0.12$ V for pH 5.9; when $E'_6 = -0.11$ V and a similar value of Q are used, the resulting potential is 0.06 V at pH 5.

These rough estimates suggest that E_6 is even smaller below pH 5, which translates to a lower reactivity of e_{cb}^- toward CCl_3F and a decrease in efficiency of step 6. This favors termination via step 10 because the driving force needed for reducing trihalomethyl radicals is less than that for the reduction of the parent compounds.[27] Hence, the P.E.$(F^-)_i$ value measured at pH 4 represents the combined contributions of steps 9 and 10. In addition, the contributions of these reactions and of step 11 to the overall yield of Cl^- can no longer be neglected, invalidating the steady-state assumptions made to derive eq 12. Differences in the driving force of step 6 can account, in part, for the change in P.E.$(Cl^-)_i$ at pH > 4 illustrated in Figure 4, where CCl_3F is reduced by both e_{cb}^- and $^{\bullet}CO_2^-$, but step 7 is probably faster than step 6. At pH < 5 the Freon is reduced primarily via step 7 whereas reaction 6 must compete with steps 2 and 10. Diversion of electrons into the latter reaction channels lowers the efficiency of step 6, limiting the chain length and decreasing P.E.$(Cl^-)_i$ while P.E.$(F^-)_i$ increases.

Analysis of the initial rate data using steady-state methods assumes that Cl^- and F^- are formed largely via propagations and terminations that proceed in the double-layer region. However, the declines in $r(Cl^-)$ at longer times (Figures 1 and 4) are incompatible with a mechanism based only on homogeneous steps. The results of Figure 5 suggest that the concentrations of chain carriers decrease as photolysis proceeds because lowering $[^{\bullet}CO_2^-]_{ss}$ and $[^{\bullet}CCl_2F]_{ss}$ favors generation of Cl^- over F^-. Tests with data collected at 10 min of photolysis (the longest time for which the derived expressions yield self-consistent results) confirm this suspicion. Using the ζ_i, $r(Cl^-)_i$, and $r(F^-)_i$ values obtained at pH 5.9 in eqs 13, 15, 16, and 17 (5.6×10^{-3}, 1.9×10^{-6} M s^{-1}, and 6.1×10^{-9} M s^{-1}, respectively) yields $k_7 = 9.6 \times 10^4$ M^{-1} s^{-1}, $k_8 = 2.6 \times 10^3$ M^{-1} s^{-1}, and $[^{\bullet}CO_2^-]_{ss} = [^{\bullet}CCl_2F]_{ss} = 2.5 \times 10^{-9}$ M. The large change in ζ_i from 0.18 to 5.6×10^{-3} after 10 min indicates that step 2 becomes more significant as irradiation continues. Faster charge carrier recombinations are expected when electrons accumulate in the TiO_2 particles.[38] Electron accumulation takes place under conditions favoring injection of electrons into the oxide via step 5, which has an adverse cascading effect on the Freon reduction since the strongly reducing $^{\bullet}CO_2^-$ radical transforms into the weaker reductant e_{cb}^-. Acceleration of step 2 lowers the rate of step 4 and also the amount of radicals able to participate in step 7.

The impact of step 5 varies with $[H^+]$ because electron injection by $^{\bullet}CO_2^-$ radicals present in the double layer is less probable at pH 8, where the TiO_2 surface is negatively charged, but increases below pzc as the surface turns positively charged. This interpretation accounts for the falling rates of Cl^- formation during photolysis at pH $\geq$ 5.9 shown in the inset of Figure 4. The larger decreases in $r(Cl^-)$ noticed at pH 5.9 result from a higher efficiency of step 5 combined with the lower driving force for step 6 compared with the E_6 value for pH 8 (0.22 V). On the other hand, HCO_2^- is bound to the oxide below pzc, where step 4 is mainly a surface reaction. Thus, most of the $^{\bullet}CO_2^-$ radicals remain adsorbed on the oxide; even radicals formed in the double layer are attracted to the particles, making step 5 far more probable. This process is particularly detrimental to the photoreaction at pH < 5 because of the lower driving force of step 6 and is probably the reason for the slower Cl^- formation at pH 4 shown in the inset of Figure 4. Step 5 is expected to yield some trapped electrons, which are known to raise the Fermi level of TiO_2,[39] augmenting the driving force of step 6. This effect may explain the increases in $r(Cl^-)$ during extended illuminations at pH 4 depicted in the inset of Figure 4.

The efficient conversion of the undesirable CFC 11 to HCFC 21 using semiconductor-initiated chain reductions has been demonstrated in this study. CCl_3F is transformed via reductions much faster than those of CFC 113, with long chains occurring at high light intensities. Despite the coexistence of aqueous and CFC phases, the kinetic data can be understood in terms of simple steady-state assumptions combined with well-known interfacial processes of TiO_2. Subsequent reports will show that these concepts are useful for rationalizing the improvements in reaction efficiency induced by O_2 and by the presence of the CFC phase.

Acknowledgment. We thank Degussa for a gift of TiO_2 P-25 samples, and G. Goodloe for his help with GC−MS measurements. We are grateful to the U.S. Navy for supporting R.L.C. through the CIVINS program and to NTC for partial support of this research.

References and Notes

(1) Li, Y. In *Molecular and Supramolecular Photochemistry 1 (Organic Photochemistry)*; Ramamurthy, V., Schanze, K. S., Eds.; Marcel Dekker: New York, 1997; p 295.

(2) Mills, A.; Le Hunte, G. *J. Photochem. Photobiol., A* **1997**, *108*, 1.

(3) Kamat, P. V.; Vinodgopal, K. In *Molecular and Supramolecular Photochemistry 2 (Organic and Inorganic Photochemistry)*; Ramamurthy, V., Schanze, K. S., Eds.; Marcel Dekker: New York, 1998; p 307.

(4) Hoffmann, M. R.; Martin, S. T.; Choi, W.; Bahnemann, D. W. *Chem. Rev.* **1995**, *95*, 69.

(5) Serpone, N.; Terzian, R.; Minero, C.; Pelizzetti, E. In *Photosensitive Metal-Organic Systems*; Kutal, C., Serpone, N., Eds.; Advances in Chemistry Series 238; American Chemical Society: Washington DC, 1993; p 281.

(6) (a) Micic, O. I.; Zhang, Y.; Cromak, K. R.; Trifunac, A. D.; Thurnauer, M. C. *J. Phys. Chem.* **1993**, *97*, 7277. (b) Lawless, D.; Serpone, N.; Meisel, D. *J. Phys. Chem.* **1991**, *95*, 5166.

(7) (a) Wada, Y.; Yin, H.; Kitamura, T.; Yanagida, S. *J. Chem Soc., Chem. Commun.* **1998**, 2683. (b) Kuhler, R. J.; Santo, G. A.; Caudill, T. C.; Betterton, E. A.; Arnold, R. G. *Environ. Sci. Technol.* **1993**, *27*, 2104. (c) Bahnemann, D. W.; Mönig, J.; Chapman, R. *J. Phys. Chem.* **1987**, *91*, 3782.

(8) (a) Choi, W.; Hoffmann, M. R. *Environ. Sci. Technol.* **1997**, *31*, 89. (b) Choi, W.; Hoffmann, M. R. *J. Phys. Chem.* **1996**, *100*, 2161. (c) Choi, W.; Hoffmann, M. R. *Environ. Sci. Technol.* **1995**, *29*, 1646.

(9) (a) Calza, P.; Minero, C.; Pelizzetti, E. *Environ. Sci. Technol.* **1997**, *31*, 2198. (b) Hilgendorff, M.; Hilgendorff, M.; Bahnemann, D. W. *J. Adv. Oxid. Technol.* **1996**, *1*, 35.

(10) (a) Huang, Z.-Y.; Barber, T.; Mills, G.; Morris, M.-B. *J. Phys. Chem.* **1994**, *98*, 12746. (b) Popovic, I. G.; Katsikas, L.; Müller, U.; Velickovic, J. S.; Weller, H. *Macromol. Chem. Phys.* **1994**, *195*, 889. (c) Hoffman, A. J.; Yee, H.; Mills, G.; Hoffmann, M. R. *J. Phys. Chem.* **1992**,

96, 5540. (d) Hoffman, A. J.; Mills, G.; Yee, H.; Hoffmann, M. R. *J. Phys. Chem*. **1992**, *96*, 5546.

(11) Al-Ekabi, H.; de Mayo, P. *J. Phys. Chem*. **1986**, *90*, 4075.

(12) Okada, K.; Hisamitsu, K.; Takashi, Y.; Hanaoka, T.; Miyashi, T.; Mukai, T. *Tetrahedron Lett*. **1984**, *25*, 5311.

(13) Sahyun, M. R. V.; Serpone, N. *Langmuir* **1997**, *13*, 5082.

(14) (a) Evans, R.; Nesyto, E.; Radlowski, C.; Sherman, W. V. *J. Phys. Chem*. **1971**, *75*, 2762. (b) Radlowski, C.; Sherman, W. V. *J. Phys. Chem*. **1970**, *74*, 3043. (c) Sherman, W. V. *J. Phys. Chem*. **1968**, *72*, 2287.

(15) Bullock, G.; Cooper, R. *Trans. Faraday Soc*. **1970**, *66*, 2055.

(16) Horowitz, A. In *The Chemistry of Functional Groups, Supplement D, Part 1*; Patai, S., Rappoport, Z., Eds.; J. Wiley: Chichester, 1983; p 369.

(17) (a) Mönig, J.; Asmus, K.-D. *J. Chem. Soc., Perkin Trans. 2* **1984**, 2057. (b) Köster, R.; Asmus, K.-D. *Z. Naturforsch.* **1971**, *26b*, 1104.

(18) (a) Hu, C.-M.; Tu, M.-H. *J. Fluorine Chem*. **1991**, *55*, 105. (b) Alfassi, Z. B.; Heusinger, H. *Radiat. Phys. Chem*. **1983**, *22*, 995.

(19) Ravishankara, A. R.; Lovejoy, E. R. *J. Chem. Soc., Faraday Trans.* **1994**, *90*, 2159.

(20) Weaver, S.; Mills, G. *J. Phys. Chem. B* **1997**, *101*, 3769.

(21) Stark, J.; Rabani, J. *J. Phys. Chem. B* **1999**, *103*, 8524.

(22) Shen, T.-L.; Wooldridge, P. J.; Molina, M. J. In *Composition, Chemistry and Climate of the Atmosphere*; Singh, H. B., Ed.; Van Nostrand Reinhold: New York, 1995; Chapter 12.

(23) Stanbury, D. M. *Adv. Inorg. Chem*. **1989**, *33*, 69.

(24) Heller, H. G.; Langan, J. R. *J. Chem. Soc., Perkin Trans. 2* **1981**, 341.

(25) Horvath, A. L. *Halogenated Hydrocarbons: Solubility−Miscibility with Water*; Marcel Dekker: New York, 1982; pp 661−710.

(26) (a) Cunningham, J.; Al-Sayyed, G.; Srijarani, S. In *Aquatic and Surface Photochemistry*; Helz, G. R., Zepp, R. G., Crosby, D. G., Eds.; CRC Press: Boca Raton, FL, 1994; p 317. (b) Turchi, C. S.; Ollis, D. F. *J. Catal*. **1990**, *122*, 178.

(27) Hawley, M. D. In *Encyclopedia of Electrochemistry of the Elements*; Bard, A. J., Lund, H., Eds.; Marcel Dekker: New York, 1980; Vol. XIV, p 1.

(28) Augustynski, J. In *Structure and Bonding. Solid Materials*; Springer-Verlag: Berlin, 1988; Vol. 69, p 1.

(29) Huyser, E. S. *Free-Radical Chain Reactions*; Wiley-Interscience: New York, 1970; Chapter 3.

(30) Balkas, T. I.; Fendler, J. H.; Schuler, R. H. *J. Phys. Chem*. **1971**, *75*, 455.

(31) Martens, R.; von Sonntag, C.; Lind, J.; Merenyi, G. *Angew. Chem., Int. Ed. Engl*. **1994**, *33*, 1259.

(32) (a) Akratopulu, K. Ch.; Kordulis, C.; Lycourghiotis, A. *J. Chem. Soc., Faraday Trans*. **1990**, *96*, 3437. (b) Jaffrezic-Renault, N.; Pichat, P.; Foissy, A.; Mercier, R. *J. Phys. Chem.* **1986**, *90*, 2733. (c) Janssen, M. J. G.; Stein, H. N. *J. Colloid Interface Sci*. **1986**, *109*, 508.

(33) (a) Mpandou, A.; Siffert, B. *J. Colloid Interface Sci*. **1984**, *102*, 138. (b) Foissy, A.; Mpandou, A.; Lamarche, J. M.; Jaffrezic-Renault, N. *Colloids Surf*. **1982**, *5*, 363.

(34) Salinaro, A.; Emeline, A. V.; Zhao, J.; Hidaka, H.; Ryabchuk, V. K.; Serpone, N. *Pure Appl. Chem*. **1999**, *71*, 321.

(35) Ward, M. D.; White, J. R.; Bard, A. J. *J. Am. Chem. Soc*. **1983**, *105*, 27.

(36) Wang, C.-M.; Heller, A.; Gerischer, H. *J. Am. Chem. Soc*. **1992**, *114*, 5230.

(37) Sczechowski, J. G.; Koval, C. A.; Noble, R. D. *J. Photochem. Photobiol., A* **1993**, *74*, 273.

(38) Gerischer, H.; Heller, A. *J. Phys. Chem*. **1991**, *95*, 5261.

(39) Rajh, T.; Ostafin, A. E.; Micic, O. I.; Tiede, D. M.; Thurnauer, M. C. *J. Phys. Chem*. **1996**, *100*, 4538.